4th International Symposium on Geotechnical Engineering
for the Preservation of Monuments and Historic Sites

TC301-2026-32

Assessment of Stability Conditions for a Large Block Overhanging a Nabataean Archaeological Well at the UNESCO Site of HEGRA – KSA

E. Lusini[1], D. Boldini[2], D. Spizzichino[3] and C. Margottini[4]

[1]*Research Associate, Sapienza University of Rome, Rome, Italy, email: edoardo.lusini@uniroma1.it*

[2]*Associate Professor, Sapienza University of Rome, Rome, Italy, email: daniela.boldini@uniroma1.it*

[3]*Researcher, ISPRA, Department for Geological Survey of Italy, Rome, Italy, email: daniele.spizzichino@isprambiente.it*

[4]*Adjunct Professor, UNESCO Chair on the Prevention and Sustainable Management of Geo-Hydrological Hazards, University of Florence, Firenze, Italy, email: claudio.margottini@gmail.com*

ABSTRACT

This paper analyses the stability of a potentially hazardous rock block above a Nabataean archaeological well at Hegra, near the Al-Ula oasis in the Kingdom of Saudi Arabia, and proposes low-impact intervention measures. The final design aims to preserve cultural heritage while ensuring safety during archaeological surveys and restoration works. The site is characterised by layered sandstone formations with variable strength, resulting in a banded erosion pattern that affects rock stability. A detailed 3D model of the area was generated using UAV photogrammetry, accurately reproducing the geometry of both the block and the slope. In-situ and laboratory tests on collected samples provided the required strength and deformability parameters. The developed model was used for static and pseudo-static analyses of increasing complexity, including limit-equilibrium assessments and 3D FEM stress-strain simulations, in which an elasto-plastic interface reproduced joint behaviour. Cohesive strength was progressively reduced to simulate the degradation of rock bridges, yielding a conservative unit safety factor under static loading. The proposed intervention method consists of passive low-impact dowels, modelled as embedded beam elements in the simulations. This study outlines a methodological approach suitable for comparable geological and geomechanical contexts and provides the first comprehensive physical and mechanical characterisation of local sandstone at site scale.

INTRODUCTION

Weak-rock monuments represent an important component of the world's cultural heritage (e.g. Petra in Jordan, Lalibela in Ethiopia) and Madâin Sâlih near Al-Ula in Saudi Arabia is among these. Madâin Sâlih, located about 22 km from Al-Ula, was historically known as Al-Hijr or Hegra and is the second most important centre of the Nabataean civilisation (312 BC-106 AD) after their capital, Petra in Jordan. The Nabateans carved more than one hundred monumental tombs, religious structures and wells, enriched with inscriptions and elaborately decorated façades, all excavated in Lower Paleozoic sandstones (Beni et al., 2023). Most of the archaeological remains date back to the Nabatean kingdom (1st century AD). Evidence of Dadanite and Lihyanite occupation before the Nabataeans, and of Roman presence afterwards, is also preserved.
In 2008, UNESCO proclaimed Madâin Sâlih as Saudi Arabia's first World Heritage Site (Margottini et al., 2016). It was recognised for the exceptional state of preservation of its monuments from late antiquity, in particular the 131 rock-cut monumental tombs characterised by their richly ornamented façades (Gallego et al., 2023).

GEOLOGICHAL AND GEOMORFOLOGICAL SETTING

The main formations exposed in the area are the Siq, Quweira and Saq sandstones (Husseini, 1990; Tuvia & Sneh, 2002). Due to its structural configuration, the Siq sandstone predominantly crops out in Al-Ula, to the south, whereas in the Hegra area the main exposed unit is the Quweira sandstone. The

unstable rock block examined in this work lies within the archaeological site of Hegra and is entirely within the Quweira sandstone (Figure 1). The investigated block is intact at visual inspection, while the surrounding rock slopes does not present through-going fractures which may lead to further detachments.
The unstable block is interpreted as a translational rockslide according to Hungr et al. (2013), moving along a pre-existing planar surface, a mechanism typical of dip-slope conditions where discontinuities are sub-parallel to the slope face (Gallego et al., 2022).

Figure 1. *View of the unstable rock block analysed in this study.*

GEOMECHANICAL CHARACTERISATION

The rock material was characterised through laboratory testing carried out at Sapienza University of Rome (Italy). Specimens were obtained from five blocks collected at the investigated site, close to the block of interest. Following a preliminary assessment of their dimensions, mass, porosity, and dynamic stiffness, the cored specimens were subjected to uniaxial compression, triaxial and Brazilian tests under both dry and wet conditions to evaluate the influence of saturation on rock strength. Table 1 summarises the average values of the physical and mechanical parameters. These values are consistent with the results from similar tests conducted on the same material at the University of Milan Bicocca during the 2021 – 2022 field surveys (Gallego et al., 2023).
The properties of the rock joints were determined during in situ surveys conducted in March 2024 (Table 2). Several rebound tests with a Schmidt hammer were performed on both natural surfaces and an artificially polished surface prepared on site. The Schmidt hammer results indicate an average *JCS* of 35 MPa, only slightly lower than the *UCS* values determined in laboratory tests on dry specimens, suggesting minimal alteration of the rock wall material. A Geological Strength Index (*GSI*) of 69 was estimated for the rock-mass, primarily due to the generally wide spacing of joints.

Table 1. *Values of the physical and mechanical parameters of the Quweira sandstone.*

Parameters	Value	Unit
Porosity (n)	17.0	%
Dry unit volume weight (γ_{dry})	21.5	kN/m^3
P-wave velocity (V_P)	2.56	km/s
S-wave velocity (V_S)	1.63	km/s
Dry uniaxial compressive strength (UCS_{dry})	40.3	MPa
Wet uniaxial compressive strength (UCS_{wet})	27.2	MPa
Dry tensile strength ($\sigma_{t,dry}$)	3.4	MPa
Secant Young's modulus at 50% of peak load ($E_{s,50}$)	7.8	GPa
Tangent Young's modulus at 50% of peak load ($E_{s,50}$)	11.1	GPa

Table 2. *Mechanical properties of the joints (*Schmidt hammer oriented* 90° downward).

Parameters	Value	Unit
Joint roughness coefficient (*JRC*)	8-10	-
Schmidt hammer rebound* on natural surfaces (*r*)	19.1	-
Schmidt hammer rebound* on polished surfaces (*R*)	20.5	-
Joint coefficient strength (*JCS*)	35	MPa
Basic friction angle from tilting tests (φ_b)	35	°
Residual friction angle (φ_r)	33.6	°

SEISMICITY OF THE AREA

From a recent site-specific seismotectonic study (Ezzelarab et al., 2025), the uniform hazard response spectra (UHRS) in the horizontal direction specific for Al'Ula were available for different return periods (*TR*) and for a critical damping ratio of 5%. Peak ground acceleration (*PGA*) values of 0.091 g and 0.23 g were obtained for *TR* = 475 y and *TR* = 2475 y, respectively. According to Eurocode 8, these return periods correspond to the Significant Damage (SD) and the Near Collapse (NC) limit states, respectively, for ordinary buildings (Importance Class II). In the present study, a *PGA* value of 0.2 g was adopted; this may be regarded as conservative, as design codes typically consider compliance with the SD limit state to be sufficient.

3D GEOMETRY RECONSTRUCTION

The slope geometry was reconstructed starting from a detailed point cloud of the slope, acquired by UAV photogrammetry with centimetric resolution (Factum Foundation, 2023).
After an initial segmentation step to isolate the area of interest, the dataset was refined within CloudCompare© software through the Noise Filter tool to remove outliers. The reduced point cloud was then exported to Rhinoceros CAD© software, where the topographic surface of the slope, including the overhanging block, was reconstructed as a single NURBS surface using the Patch command. Solid volumes were subsequently generated through trimming operations in AutoCAD 3D©. The joint surface was obtained as a best-fit median plane to the trace of the joint emerging on the slope, visible in the point cloud, and was then used to separate the unstable block from the rest of the slope. The entire procedure is summarised in Figure 2.
At the end of the procedure, the main geometrical characteristics of the block were determined, including its volume V_b = 196.5 m^3, the area of the joint surface A_j = 100 m^2, and the dip and dip direction of the joint plane (68°/60°).

STABILITY ASSESSMENT

The stability of the rock block is assessed using two methods of increasing complexity, following a workflow comparable to that proposed by Spizzichino et al. (2016) and Boldini et al. (2018), while considering the full three-dimensionality of the problem.
First, a limit equilibrium analysis against planar sliding is conducted under static and pseudo-static conditions, both for the existing configuration and for a mitigation scenario incorporating passive, fully grouted dowels. Second, a finite element model is employed to simulate the same conditions and to investigate a more realistic stress–strain response of the slope.

Limit equilibrium analyses

A planar sliding mechanism along the dip of the discontinuity delimiting the block is assumed. The site investigation allowed the definition of a Barton failure criterion for the discontinuity, providing a shear strength dependent on the normal stress.
A simple comparison between the dip angle of the discontinuity (68°) and the peak friction angle derived from the Barton criterion (φ_r + 35° = 68.5°) indicates that equilibrium in static conditions can only be achieved by assuming the presence of rock bridges bonding the two walls of the joint.

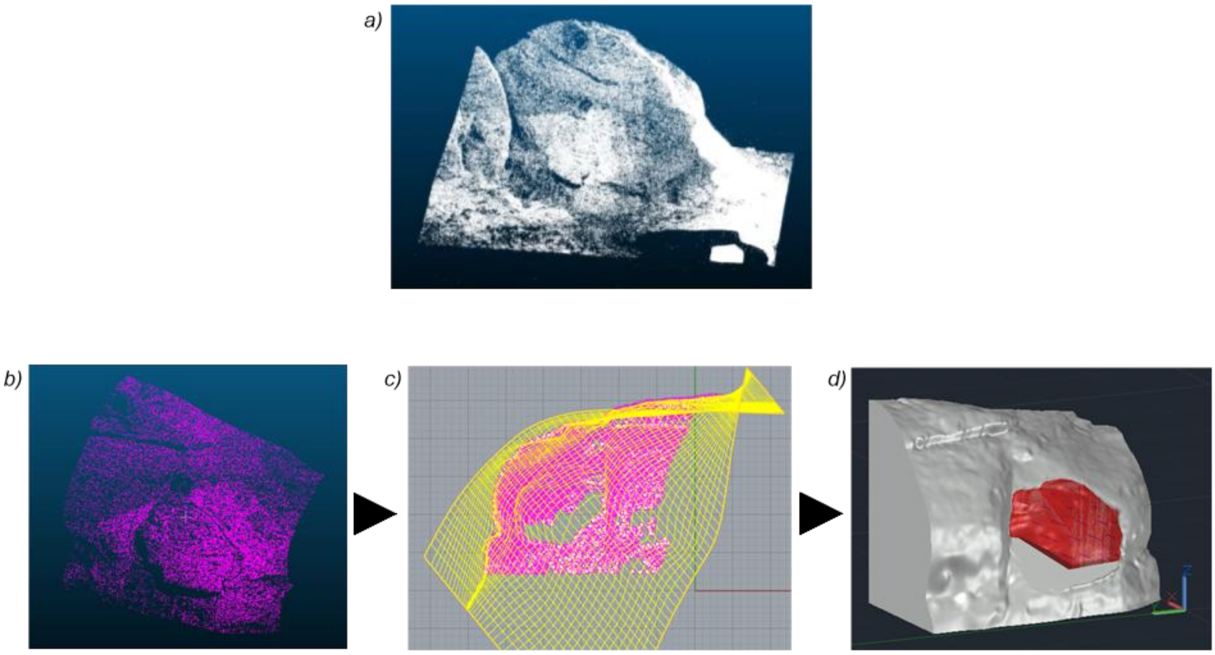

Figure 2. *UAV point cloud of the slope (Factum Foundation, 2023) (a); segmented and cleaned point cloud around the unstable block (b); NURBS interpolating surface (c); trimmed solid volumes of the slope and block (d).*

The extent of these rock bridges, being unknown, is conservatively taken as the minimum necessary to ensure equilibrium. Their contribution is incorporated into the Barton criterion in the form of a fictitious cohesion, c_{rb}, smeared across the entire contact surface of the discontinuity (Frayssines & Hantz, 2009). This approach is implemented by imposing a factor of safety FS = 1 in the equilibrium equation at failure. This latter is defined as:

$$FS = \frac{A_j\, c_{rb} + N \tan\left(\varphi_r + JRC \log_{10} \dfrac{JCS}{\sigma_n} \right)}{T} \tag{1}$$

where N and T are the tangential and normal components of the self-weight acting on the joint plane, σ_n is the average normal stress on the joint plane, and JCS is the joint wall compressive strength, assumed as equal to 23.8 MPa. This value is derived by scaling the Schmidt hammer results, considering the reduction in strength due to saturation of the material, as observed in laboratory *UCS* tests.
The resulting cohesion contribution c_{rb} offered by rock bridges is consequently estimated at 10.5 kPa.
The block stability is then evaluated in seismic conditions, through a pseudo static approach, applying mass-proportional forces in the horizontal and vertical directions. The horizontal and vertical equivalent seismic coefficients are calculated according to Eurocode 8 procedure as:

$$k_H = 0.5 \frac{a_g}{g} S \tag{2}$$

$$k_V = \pm 0.5\, k_H \tag{3}$$

where k_H and k_v are horizontal and vertical seismic coefficients (with the sign of the vertical coefficient depending on the most severe condition between upward and downward directed equivalent seismic forces, unknown *a priori*), a_g = 0.2 g is the expected *PGA* at the site, g is the gravity acceleration and S is a factor accounting for combined topographic and stratigraphic amplification effects. No stratigraphic amplification is expected in rock mass outcrops, so the factor S coincides with the only topographic factor S_T, which is conservatively assumed as equal to 1.4 according to Eurocode 8, compatibly with isolated cliffs (≥ 1.2) or ridges with slope inclination greater the 30° (≥ 1.4).

Equation (1) can still be used to calculate the *FS*, provided that the values of *N* and *T* are updated according to the following equations.

$$N = W\cos\psi_g \pm k_v W\cos\psi_g - k_h W\sin\psi_g \tag{4}$$

$$T = W\sin\psi_g \pm k_v W\sin\psi_g + k_h W\cos\psi_g \tag{5}$$

where *W* is the self-weight and ψ_g is the average inclination of the discontinuity plane. The factors of safety obtained from the pseudo-static analyses are 0.73 and 0.74 for the downward and upward vertical components of the equivalent seismic force, respectively.

To ensure the safety of the archaeological area, compatible with intensive touristic use, a mitigation measure is deemed necessary. The factor of safety in pseudo static conditions increases to *FS* = 1.55 through 19 passive dowels oriented normal to the slope face, with an approximate spacing of 2 m. The selected dowels are 28 mm in diameter, with a minimum characteristic yield stress of σ_Y = 430 MPa. Equation 1 can be reformulated to account for the equivalent cohesive contribution of each dowel c_b as:

$$FS = \frac{A_j\, c_{rb} + N\tan\left(\varphi_r + JRC\log_{10}\dfrac{JCS}{\sigma_n}\right) + A_j\, n_b c_b}{T} \tag{6}$$

where n_b = 19 is the number of dowels. The cohesive contribution from the rock bridges, c_{rb}, can be conservatively assumed to be zero, considering that some level of slip is required to mobilise the dowel resistance, which is not acceptable for the intact rock.

The cohesive contribution of the dowels can be calculated following Panet (1987), by assuming sliding along the discontinuity as the failure mechanism:

$$c_b = \frac{R_b\left[\cos(\beta+\theta)\tan\varphi + sen(\beta+\theta)\right]}{A_j} \tag{7}$$

where R_b is the resisting force in the single dowel section at the crossing with the joint surface, β is its inclination with respect to the dowel axis, θ = 25° is the dowel inclination with respect to the joint normal, and φ = 33.6° is the residual friction angle from Barton criterion. The force R_b and its orientation β can be calculated based on the principle of maximum work (Ribacchi et al., 1995). They depend on the angle 90 – (θ-*i*) between the dowel axis and the displacement vector *u*, which describes the relative movement between the two joint surfaces and is considered inclined at an angle *i* = 14° with respect to the joint dip, equal to half of the peak dilatancy angle determined from the Barton criterion. For the block under examination, they are estimated in R_b = 246 kN and β = 7.1°. Considering that the most critical failure mechanism is given by the formation of plastic hinges, and not by the shear failure of the dowels, the strength contribution of the reinforcement is equal to $C_{be} = A_j\ n_b\ c_b$ = 4997 kN. The plastic hinge formation mechanism is governed by the rock crushing strength. The value here adopted is equal to 3 times the Joint Compression Strength (*JCS*) according to referenced literature (Ribacchi et al., 1995); its possible variability in the interval between *JCS* and 4 times its value is assessed and does not alter the most critical failure mechanism, with negligible influence on the *FS*.

The dowels are also checked against possible pull-out. Following British Standard 8081 (1989), the pull-out strength at the rock-mortar interface was assumed equal to one-tenth of the uniaxial compressive strength of the rock. The resulting shear stress is 2.38 MPa, which for a dowel length of 2.0 m embedded in the stable portion of slope corresponds to a pull-out resistance of 690 kN. This is much higher than the tensile force acting on the dowel, equal to 244 kN. As for the potential pull-out at the mortar–steel interface, the same British Standard recommends a minimum embedment length of 40 times the dowel diameter. For a 28 mm dowel, this corresponds to 1.12 m, considerably less than the length used in the present design.

Numerical analyses

The entire portion of the slope shown in Figure 2c is modelled in PLAXIS 3D©. The finite-element model and the corresponding computational mesh are shown in Figure 3.

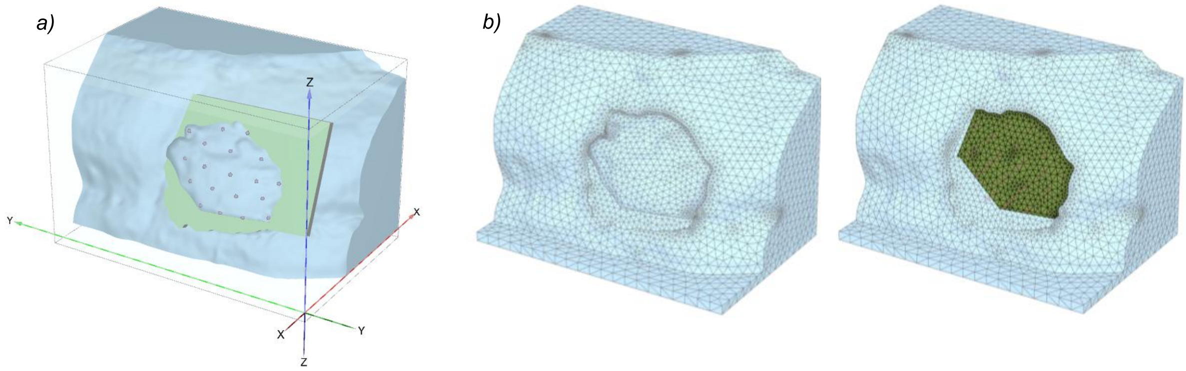

Figure 3. *FEM model of the slope, including the overhanging block, the joint surface, and the dowels (a), and the computational mesh (b).*

The stiffness and strength parameters adopted for the rock and joint are summarised in Table 3, while those used for the dowels are reported in Table 4.
Because the Barton criterion is not implemented in PLAXIS for interface elements, it is linearised into an equivalent Mohr–Coulomb criterion over the normal stress range 0–1300 kPa, resulting in an apparent cohesion of 15 kPa and a friction angle of 49°. A final step of analysis is performed with residual strength parameters along the interface (φ_j = 33.6°, ψ_j = 0° and c_j = 0 kPa).The elastic stiffness of the joint is assigned with the aim to represent physical joint compliance and not a mere hard contact, adopting typical literature values for the tangential stiffness (k_s = 300 MPa/m) and the normal stiffness (k_n = 5 k_s). In order to quantify the influence of the assumed interface stiffness on the results, a sensitivity analysis is performed, considering a multiplying factor of 5 and 10 the selected values.
The passive reinforcement is modelled using elasto-plastic embedded beam elements, each representing a fully grouted dowel. The dowels are 6 m long to ensure adequate anchorage within the stable portion of the slope and are arranged with an average spacing of 2 m. Each embedded beam is linked to the surrounding continuum by an interface, whose maximum shear resistance can be controlled by specifying a pull-out strength per metre.

Table 3. *Mohr-Coulomb elasto-plastic parameters assumed in the analysis for the rock and the joint.*

Rock block	Value	Unit	Joint - Interface	Value	Unit
Unit weight (γ_r)	23.5	kN/m^3	Normal stiffness (k_n)	1500	MPa/m
Young's modulus (E_r)	8.0	GPa	Tangential stiffness (k_s)	300	MPa/m
Poisson coefficient (ν_r)	0.25	-	Cohesion (c_j)	15	kPa
Cohesion (c_r)	7.5	MPa	Friction angle (φ_j)	49	°
Friction angle (φ_r)	46	°	Dilatancy angle (ψ_j)	14	°
Dilatancy angle (ψ)	23	°	Tensile cut-off ($\sigma_{t,j}$)	0	kPa
Tensile cut-off ($\sigma_{t,r}$)	3.4	MPa			

Table 4. *Elasto-plastic parameters adopted for the embedded beam elements representing the dowels.*

Dowels - Embedded beam	Value	Unit		Value	Unit
Unit weight (γ)	78.5	kN/m^3	Yield stress (σ_Y)	430	MPa
Diameter (D)	28	mm	Axial skin resistance (T_{max})	345	kN/m
Young's modulus (E)	200.0	GPa			

A static analysis is initially carried out. In the first stage, an isotropic stress state is initialised within a 20 × 30 × 20 m volume, representing a portion of the Quweira formation prior to any erosional processes. The second stage aimes to simulate erosion through the progressive retreat of the scarp, a mechanism typical of arid environments, by deactivating solid clusters and thereby exposing the current steep slope face. During this phase, the interface representing the joint is assigned the same mechanical properties as the intact rock. In the subsequent stage, joint properties are applied to the interface together with an additional cohesive component sufficient to ensure stability (c_j = 30 kPa). This cohesion is then progressively reduced to c_j = 22.9 kPa to approach limit-equilibrium conditions (Matsui & San, 1992; Dawson et al., 1999), corresponding to full plasticisation along the interface. This residual value implies a rock-bridge contribution of c_{rb} = 7.9 kPa, considering the 15 kPa of apparent cohesion resulting from the linearisation of the Barton criterion. This value is slightly lower than that estimated through the limit-equilibrium method (10.5 kPa).

To assess the effects of dowel installation, the 19 embedded beams are subsequently activated simultaneously, and the cohesion along the discontinuity is further reduced to 15 kPa, corresponding to the intercept of the linearised Barton criterion and therefore not representing any true cohesive contribution, as assumed in hand calculations. At this stage, the pseudo-static forces in the horizontal and vertical directions are applied to the model as body forces, analogous to gravity, to simulate seismic excitation.

None of the dowels has reached the two-hinge plasticisation at this stage. The global shear demand on the dowels can be estimated in a mobilised tangential contribution T_{mob} = 31.6 kN, while the normal mobilised force results as equal to N_{mob} = 742.9 kN, with a β angle of 2.4°. The corresponding equivalent cohesive contribution of the system of dowels can be estimated in C_{be} = 757.4 kN, one tenth of the value obtained in the limit-equilibrium hand calculations. In the final step of analysis with residual strength parameters this cohesive contribution raised to C_{be} = 1503.6 kN, with only one dowel plasticised.

The assumption regarding the interface stiffness has a modest contribution to the global demand on the dowel system, resulting in C_{be} = 725.6 kN for the interface 5-times stiffened, and C_{be} = 716.9 kN for the 10-times stiffened, with a percent reduction of 4.2% and 5.3% respectively.

Along the joint surface, tendency towards toppling is evident, indicating a more complex mechanism than the pure sliding assumed in the limit-equilibrium hand calculations (Figure 4a and 4c). Except for a band at the base reaching shear failure (Figure 4b), most of the surface exhibits tension cut-off plastic points (Figure 4d).

To quantify the safety margin, the yield stress of the dowels is progressively reduced in successive calculation steps until plastic hinges has formed in all dowels (Figure 4e and 4f). This condition is reached when the yield stress has been reduced to 23% of its nominal value. The ratio between the nominal yield stress and the reduced value at which all dowels yield gives a value of 4.35, substantially higher than the ratio between the number of dowels needed according to the limit-equilibrium approach and the number calculated if a factor of safety of 1 has been adopted (19/9 = 2.11).

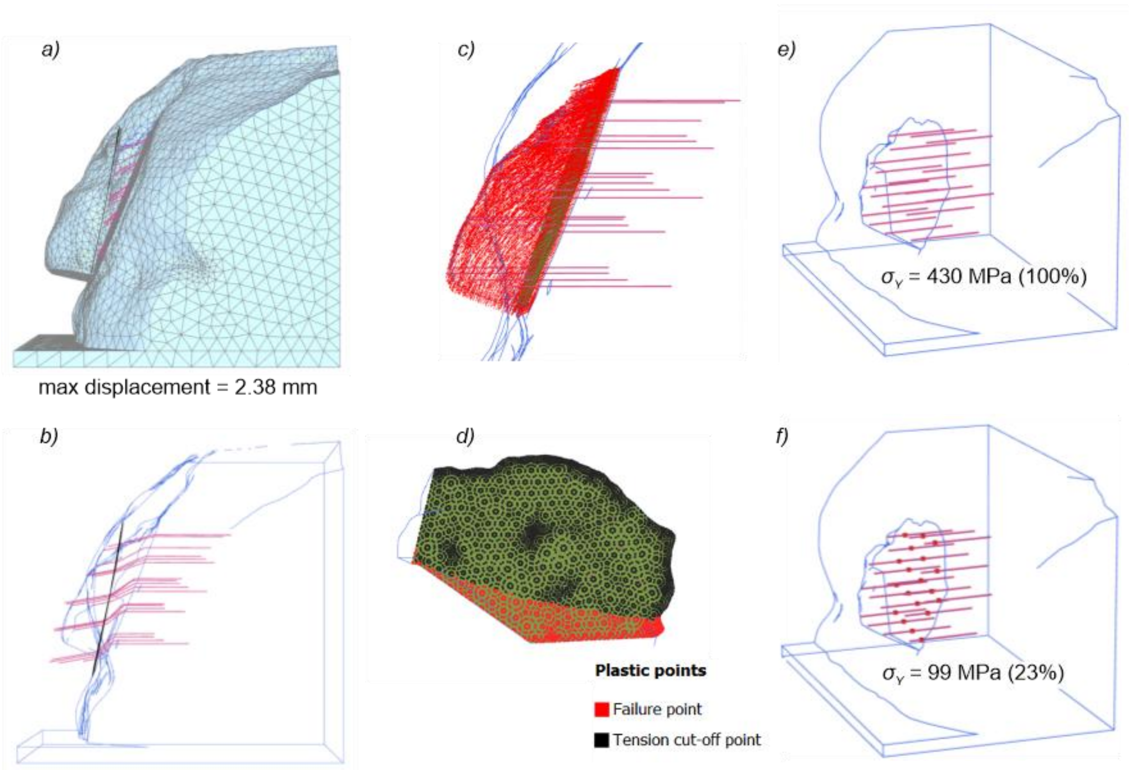

Figure 4. *Deformed mesh (× 1000) (a); deformed dowels (× 1000) (b); total displacements (× 200) (c); plastic points along the joint surface (d); plastic points in the dowels for the nominal yield stress (e); and the reduced at 23% of the nominal value (f).*

Main results of the performed analyses are briefly summarised in Table 5. The considerable discrepancy between limit equilibrium and FEM calculations in presence of dowels may be attributed to the finite element mesh density, which is likely insufficient to capture the development of plastic hinges at a distance from the joint comparable to the dowel diameter, as well as to the difference in the collapse mechanism, which in the finite element simulation also involves a toppling component.

Table 5. *Comparison between main results of limit equilibrium and finite element analyses*

Type of analysis	c_{rb} **(kPa)**	**Static *FS***	**Pseudo static *FS***		**Kinematic mechanism**
		no dowels	no dowels	with dowels (no c_{rb})	
Limit Equilibrium	10.5	1.00	0.73	1.55	pure sliding
3D FEM	7.9	1.00	collapse	4.35	toppling/sliding

CONCLUSIONS

This study presents a comprehensive geomechanical and numerical assessment of the stability of a large overhanging block at the Nabataean archaeological site of Hegra, in the Kingdom of Saudi Arabia. Limit-equilibrium analyses indicated that the block's stability relies on the presence of rock bridges, represented in the analyses by a fictitious cohesion, which, however, is not sufficient to guarantee safety under a severe seismic event. The implementation of passive fully grouted dowels ensures the necessary safety conditions, with a factor of safety of 1.55, thus allowing safe access and use of the archaeological site. The final choice of a passive intervention with dowels is driven by the archaeological context which requires a combination of several constraints: low impact intervention, simple work execution by employing local labour, durability and cost efficiency.

Three-dimensional finite-element simulations of the slope confirmed the limit-equilibrium results under static conditions while providing a more realistic representation of stress–strain behaviour across the slope and on the joint surface. The activation of 19 fully grouted passive dowels substantially increased the safety margin, with pseudo-static analyses indicating a factor of safety considerably higher than that obtained from the limit-equilibrium approach, together with a different collapse mechanism characterised by a tendency for outward rotation of the block about its base. This behaviour results in differentiated stress levels acting on the individual dowels.

A low-impact intervention, to be carried out in agreement with the site conservators, could consist of concealing the housings of the dowel head plates either with borehole plugs made from core segments obtained during drilling or with a carefully prepared mortar. In order to guarantee the durability in the delicate heritage site environment, it is advised to use only dowels manufactured from stainless steel (e.g., AISI 316), which provides enhanced resistance to corrosion in outdoor rock environments. The intervention will be accompanied by a local detailed monitoring plan for controlling potential fracture opening and slope deformation with the aim to support all the stages of work execution and, at the same time, to guarantee the safety of the whole surrounding area.

Overall, the integrated methodology, combining UAV-based geometry reconstruction, detailed geomechanical characterisation, limit-equilibrium analyses, and 3D FEM simulations, provides a robust framework for assessing rock block stability at archaeological and heritage sites, supporting the design of low-impact interventions that ensure safety while preserving cultural heritage.

ACKNOWLEDGEMENTS

The field work was funded and supported by the French Agency for Al-Ula Development (AFALULA), on behalf of the Royal Commission for Al-Ula (RCU). We deeply acknowledge Ingrid Perisse and Emmanuel Mille (AFALULA) and Ignacio Gallego, Myrto Tsitsinakis and Rut Ballesteros (RCU).

REFERENCES

Beni, T., Boldini, D., Crosta, G.B., Frodella, W., Gallego, J.I., Lusini, E., Margottini, C., & Spizzichino, D. (2023). Rock instabilities at the archaeological site of Dadan (Kingdom of Saudi Arabia). Landslides, 20, 2455-2478.

Boldini, D., Guido, G. L., Margottini, C., & Spizzichino, D. (2018). Stability analysis of a large-volume block in the historical rock-cut city of Vardzia (Georgia). Rock Mechanics and Rock Engineering, 51(1), 341–349.

British Standard 8081 (1989). BS 8081: Code of practice for ground anchorages.

Dawson, E. M., Roth, W. H., & Drescher, A. (1999). Slope stability analysis by strength reduction. Géotechnique, 49(6), 835–840.

Ezzelarab, M., Abdelfattah, A., Bamousa, A. O., Alzharani, H., & Oommen, T. (2025). Unveiling the seismic hazard to Al-Madinah region, Western Saudi Arabia: A probabilistic perspective. Journal of African Earth Sciences, 232, 105798.

Frayssines, M., & Hantz, D. (2009). Modelling and back-analysing failures in steep limestone cliffs. International Journal of Rock Mechanics and Mining Sciences, 46(7), 1115–1123.

Gallego, J.I., Margottini, C., Perissé Valero, I., Spizzichino, D., Beni, T., Boldini, D., Bonometti, F., Casagli, N., Castellanza, R., Crosta, G.B., Frattini, P., Frodella, W., Gigli, G., Lusini, E., Rigamonti, S., Rusconi, G., & Vitrano, L. (2023). Rock slope instabilities affecting the AlUla archaeological sites (KSA). In: Progress in Landslide Research and Technology, I. Alcántara-Ayala et al. eds., volume 2(2), 413-429.

Gallego, J.I., Margottini, C., Spizzichino, D., Boldini, D., & Abul, J.K. (2022). Geomorphological processes and rock slope instabilities affecting the AlUla archaeological region. In: Geotechnical Engineering for the Preservation of Monuments and Historic Sites III, Lancellotta, Viggiani, Flora, de Silva & Mele eds, 456-466.

Hungr, O., Leroueil, S., & Picarelli, L. (2013). The Varnes classification of landslide types, an update. Landslides, 11, 167-194.

Husseini, M. I. (1990). The Cambro-Ordovician Arabian and adjoining plates: A glacio-eustatic model. Journal of Petroleum Geology, 13(3), 267-288.

Margottini, C., Gigli, G., Ruther, H., & Spizzichino, D. (2016). Advances in geotechnical investigations and monitoring in rupestrian settlements inscribed in the UNESCO's World Heritage List. Procedia Earth and Planetary Science, 16, 35-51.

Matsui, T., & San, K.-C. (1992). Finite element stability analysis by shear strength reduction technique. Soils and Foundations, 32(1), 59-70.

Panet, M. (1987). Reinforcement of rock foundations and slopes by passive and active anchor. In: 6th ISRM congress, (pp. 1411-1420). Montreal, Canada.

Ribacchi, R., Graziani, A., & Lembo-Fazio, A. (1995). Analisi del comportamento dei sistemi di rinforzo passivi in roccia. In: XIX Convegno Nazionale di Geotecnica, Pavia, Italy.

Spizzichino, D., Margottini, C., Chiessi, V., & Boldini, D. (2016). Assessment of the stability conditions of a large-volume sandstone block in the northern sector of the Siq of Petra. In: Landslides and Engineered Slopes – Experience, Theory and Practice, Aversa, Cascini, Picarelli & Scavia eds. CRC Press, London.

Tuvia, W., & Sneh, A. (2002). Sedimentology and paleogeography of the Late Precambrian–Early Cambrian arkosic and conglomeratic facies in the northern margins of the Arabo-Nubian Shield. Geological Survey of Israel Bulletin, 87.